Article

Polyimide nanofibers by "Green" electrospinning via aqueous solution for filtration applications

Shaohua Jiang, Haoqing Hou, Seema Agarwal, and Andreas Greiner

Just Accepted

Polyimide nanofibers by "Green" electrospinning via aqueous solution for filtration applications

Dedicated to Prof. Hans-Werner Schmidt on the occasion of this 60th birthday

Shaohua Jiang[a], Haoqing Hou[b], Seema Agarwal[a], Andreas Greiner [a]*

[a] Macromolecular Chemistry II and Bavarian Polymer Institute, University Bayreuth, Universitätsstraße 30, 95440 Bayreuth, Germany.

[b] Department of Chemistry and Chemical Engineering Jiangxi Normal University, Nanchang, 330022, China.

ABSTRACT

The use of large amounts of environmentally unfriendly, toxic, and flammable organic solvents in electrospinning of polymers puts demand on the development of new methods and formulations for making water stable hydrophobic nanofibers from water-soluble precursor solution. Electrospun polyimide (PI) nanofibers are of particular interest for a variety of applications due to their extraordinary thermal and chemical stability. However, the intermediate precursor of polyimide polyamic acid (PAA) has to be electrospun from harmful solvents like

dimethylformamide (DMF) which is a serious obstacle for technical applications of electrospun PI. This work highlights the formation of polyimide (PI) nanofibers by "green" electrospinning of ammonium salts of PAA from water. The high temperature used for imidization in the second step also removed ammonia and the template polymer by sintering giving PI nanofibers with diameter 295 ± 58 nm. The thus obtained PI nanofibers by "green" electrospinning were defined as "green" PI nanofibers. Aerosol filtration of "green" PI nanofibers showed a performance that was very similar to PI nanofibers obtained by electrospinning of PAA from DMF. Additionally, it has been shown that the "green" PI nanofibers were also suitable for the filtration of hot oil as well.

INTRODUCTION

Polyimides (PIs) are high performance polymers with excellent mechanical properties, thermal stabilities, and chemical resistance due to their rigid-rod chemical structures, which make them suitable for electronic applications, membrane, insulating materials, and aerospace industry.[1-4] Recently, PI nanofibers made by electrospinning have attracted a lot of attention for filtration, fiber reinforced composites, proton exchange membrane, and as separator for lithium-ion batteries.[5-9] Electrospinning provides continuously long nanofibers with diameter ranging from tens of nanometers to a few micrometers and electrospun fibers have been broadly applied in many fileds, including energy harvesting, environmental protection, composite materials, biomaterials, and so on.[10-13] PI electrospun nanofibers show very high tensile strength of up to 1.7 GPa, E modulus of 76 GPa,[14-15] and very good thermal and chemical resistance.[16-17] They are obtained by imidization of polyamic acid (PAA) precursor nanofibers at high temperature, which in turn are made by electrospinning from dimethylformamide (DMF) or dimethylacetamide

(DMAc). In general, the electrospinnable concentration of polymers for getting homogenous nanofibers is less than 30 wt%. This implies use of large amounts of organic solvents which might be toxic, flammable, and not environmentally friendly. Therefore, our broad aim is to replace organic solvent based electrospinning of water insoluble polymers with water based formulations. Water based electrospinning is a must for many applications such as applications in the biomedical field, agricultural applications, and wound healing and it is highly desirable for others in which the use of large amounts of toxic and flammable solvents should be avoided.[18-25] In the past, we have shown use of primary and secondary dispersions/suspensions of polyesters (hydrophobic) and amphiphilic polymers as green ways of making corresponding nanofibers.[19-24] They are generated either in situ by emulsion/suspension polymerization (primary dispersion) or by dispersing a ready-made water insoluble polymer in water. The method is applicable to many different polymers but cannot be utilized for PIs. PIs can be processed from water by making intermediate PAA precursor water soluble. There are different ways of making water soluble PAA i.e. using special starting monomers with ionic moieties or by reaction with an amine converting PAA to its carboxylate salt (PAA-salt).[26-28] Amines only with short alkyl chains such as N, N-dimethylethanol amine, triethylamine (Et$_3$N), provide water solubility to PAA whereas long alkyl chains make PAA hydrophobic and insoluble in water.[27-28] Membranes made from water soluble PAA-salt precursor show gas permeation characteristics similar to those of the corresponding membranes from organic solvents.[29] PAA-salt precursors were used for making composite fibrous membranes with SiO$_2$ or Al$_2$O$_3$ in dimethylacetamide (DMAc) as the use of PAA-salt precursor offers other advantages such as better hydrolytic stability and low thermal imidization temperature.[30]

In this work we provide "green" PI nanofibers using water as solvent. PAA precursor was spun from water in its salt form. It was solubilized in water by making ammonium salt of PAA followed by the usual imidization step. Ammonia was used for the preparation of the PAA-salt. The amine for salt formation was chosen in a way that it can be removed easily during the imidization process at high temperature. The electrospinning of polymeric salts is a challenge. We systematically investigated the electrospinning process of PAA-salt, the properties of the corresponding PI mats, and the application for room temperature and hot filtration. The present work will also be a significant step forward in the technical production of PI nanofibers under environmentally friendly conditions without use of toxic organic solvents.

EXPERIMENTAL SECTION

Materials. Pyromellitic dianhydride (PMDA, 98%, Acros Organics) and 4, 4'-oxydianiline (ODA, 99%, Acros Organics) were purified by sublimation. N, N-dimethylformamide (DMF, 99.99%, Fisher Chemical), ammonia (25 wt% in water, VWR-International), poly (ethylene oxide) (PEO, M_w = 900.000 g/mol, Acros Organics), and deionized water were used as received.

Preparation of PAA powders. 8.0096 g of ODA was first dissolved in 150 mL of DMF. Then 8.7248 g of PMDA and additional 80 mL of DMF were added to ODA. The mixture was stirred for 24 hours at 0-4 °C. At the end of the reaction, a viscous and yellow PAA solution with a concentration of 7.1 wt% was obtained. The prepared PAA solution was poured into 2.5 L of deionized water drop by drop, and the precipitated solid was filtered and dried in vacuum at 50 °C for 12 hours. The yield was 15.9 g of yellow PAA solid (yield around 95%). The intrinsic viscosity of the obtained PAA powder was 1.22 dL/g measured by Ubbelohde viscosity meter at 25 °C in DMF.

Preparation of precursor nanofibers. The water based electrospinning formulations of PAA were made in water by mixing the PAA solid, deionized water, ammonia (25 wt% in water), and PEO according to the amounts in Table S1. The applied voltage (kV) including positive and negative voltage and the flow rate (ml/h) for solutions providing good electrospinning were also listed in Table S1. The nanofibers were collected by horizontal rotating disc (rotation speed: 30 rpm; diameter: 13 cm) with a collecting distance of 20 cm between collector and electrode. For comparison purposes, PAA/DMF solution (40 wt%) for electrospinning was prepared by dissolving the PAA powder in DMF. The electrospinning of PAA/DMF solution was performed by applying voltage and flow rate of 25 kV and 0.66 ml/h, respectively.

Imidization to PI nanofibers. The PAA and PAA-salt nanofiber mats were first dried at 60 $^{\circ}$C under vacuum for 12 h and then imidized in a high-temperature furnace under N_2 with the following protocol: (a) heating up to 150 $^{\circ}$C at 10 $^{\circ}$C /min and annealing for 0.5 h to remove the residual water; (b) heating up to 250 $^{\circ}$C at 10 $^{\circ}$C /min and annealing for 1 h; (c) heating up to the final temperature of 400 $^{\circ}$C at 5 $^{\circ}$C /min and annealing for 1 h to complete the imidization process. The entire process for the preparation of PI nanofibers from organic PAA/DMF solution and water soluble precursor solution is depicted in Figure 1.
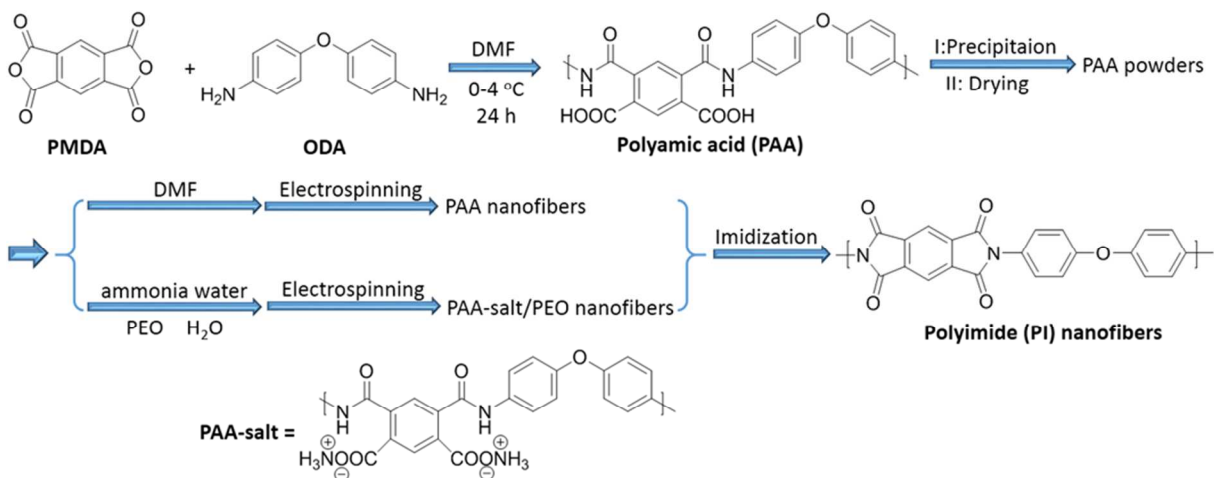
Figure 1. Schematic of preparation of "green" PI nanofibers from water-soluble precursor solution soluble PAA-slat precursor.

Preparation of filters for air and hot liquid filtration. PAA-salt and PAA nanofibers from water-soluble precursor solution and DMF solution, respectively, were deposited on the round stainless steel mesh (400 mesh, hole size 34 μm) by electrospinning using spinning formulation (sample 27 in Table S1) and PAA/DMF solutions (40 wt%). After electrospinning, nanofibers on mesh samples were imidized into PI nanofibers with the same protocol as described before. To get different coating densities of nanofibers on steel meshes, nanofibers were spun for different time intervals of 5, 10, and 20 min for air filtration and 6 min for high temperature liquid filtration. The round stainless steel meshes possess an area of 63.62 cm^2 for air filtration and 28.27 cm^2 for liquid filtration, respectively. The coating density (D, g/m^2) was calculated according to the following equation:

$$D = \frac{m_{mesh+PI} - m_{mesh}}{S_{mesh}} \quad (1)$$

Where m_{mesh}, $m_{mesh+PI}$, and S_{mesh} are the weight of the stainless steel mesh, the sum weight of the stainless steel mesh and PI, the area of the stainless steel mesh, respectively. Hot liquid filtration was performed on a self-assembled filtration set-up. The filtration mixture was prepared by mixing 1.0 mg of carbon black (particle size: 10-80 nm), 1.0 mg of Fe_2O_3 (particle size: 1-40 μm), and 500 ml of silicone oil, and was heated to 200 ^{o}C before use.

Characterization. SEM images were taken by Zeiss Leo 1530. Before scanning, the samples were all coated with 3.0 nm of platinum. Image J software was used in order to measure the fiber diameter and summarize the fiber diameter distribution. Digital microscopy photos were taken

by a digital microscope (VH-Z500). Thermal characterizations were performed on Mettler Toledo TGA/SDTA 851e at a heating rate of 10 $^{\circ}$C/Min in N_2 from 20 to 800 $^{\circ}$C. FT-IR spectra were taken by a Digilab Excalibur Series with an ATR unit MIRacle from Pike Technology. The conductivity of solutions was measured by Conductivity Meter (inoLab Terminal level 3) at room temperature. A contour plot by Origin software was made to show the espinnability with correlation of the key electrospinning parameters of the amount of ammonia and the concentration of PAA. The precise weight of all the samples was measured by OHAUS Discovery balance with readability of 0.01 mg. Mechanical properties were measured by Zwick/Roell BT1-FR 0.5TN-D14 machine. The samples for tensile test were cut into rectangular shape. The thickness and the width of the samples were measured by a screw micrometer and a vernier caliper. The stretching rate of 5 mm/min was performed during the measurement. Air filtration test was performed with a filtration system (MFP 2000, PALAS) using Di(2-ethylhexyl)-sebacate DEHS as test aerosol. A constant particle flow of 42.5 L/min was applied. The effective exposed area of the filter was 28.3 cm^2. ISO fine test dust was applied so that the particle concentration was 6000 particles per cubic centimeter and the flow rate was 0.25 m/s. Each measurement lasted 30 s. The particles generated by the machine have a particle size ranging from 0.2 to 10.0 μm. The filtration efficiency was measured from the particle concentration without filters (upstream concentration) and with filters (downstream concentration).[31] The quality factor (QF) of the filter was calculated by the following equation:[32]

$$QF = \frac{-\ln(1-\eta)}{\Delta P} \quad (2)$$

Where η, and ΔP are the filtration efficiency, the pressure drop between the up-stream and down-stream pressure, respectively.

RESULTS AND DISCUSSION

Electrospinning. The electrospinning of PAA-salt in water is a true challenge due to the very high conductivity of salt solutions. A spinning aqueous solution with 10 wt % of PAA and NH_3 possessed a conductivity of 25 mS/cm, which was 436 fold higher than that of PAA/DMF (without NH_3) solution (57.2 µS/cm). The electrospinning of PAA-salt water solution provided inhomogeneous spinning with the nanofibers vertically attracted towards the electrode and deposited on collector on turning off the voltage (Figure 2a and 2b). Therefore, a template polymer (PEO) was added in the spinning formulation which was removed during imidization temperature. To optimize the electrospinning process, 28 different solutions were prepared by changing the PAA concentration, amount of ammonia and PEO template polymer, voltage applied, and the flow rates (Table S1, Figure 3). A stable spinning process with homogenous deposition of PAA-salt nanofibers without beads from water was achieved using a formulation having 3 wt% PEO (M_w = 900,000), 10 wt% ammonia, and 10-15 wt% PAA depicted by the red area in Figure 3. The formulations with PAA and ammonia concentration in the yellow and green region (Figure 3) although provided stable electrospinning process but inhomogeneous nanofibers and nanofibers with a very small amount of beads were obtained. In these areas, both the concentrations of ammonia and PAA powders were varied from 5 to 25 wt%. The worse electrospinning process was found in pink and blue areas, where discontinuous electrospinning process and nanofibers with many beads were obtained.
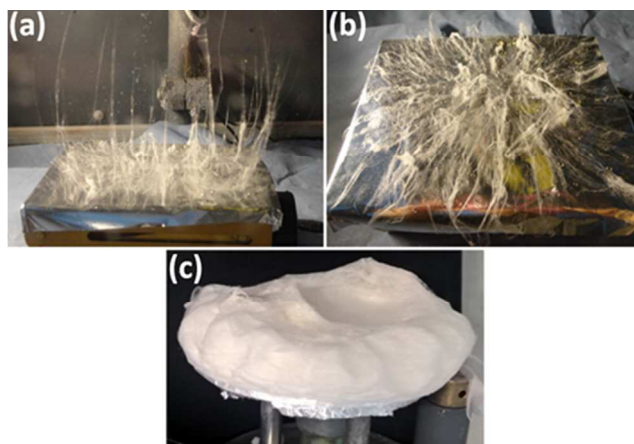
Figure 2. Electrospinning of PAA-salt/water solution when high voltage was on (a) and off (b) for sample 3. Porous and fluffy PAA-salt nanofibers electrospun from sample 27 (c).
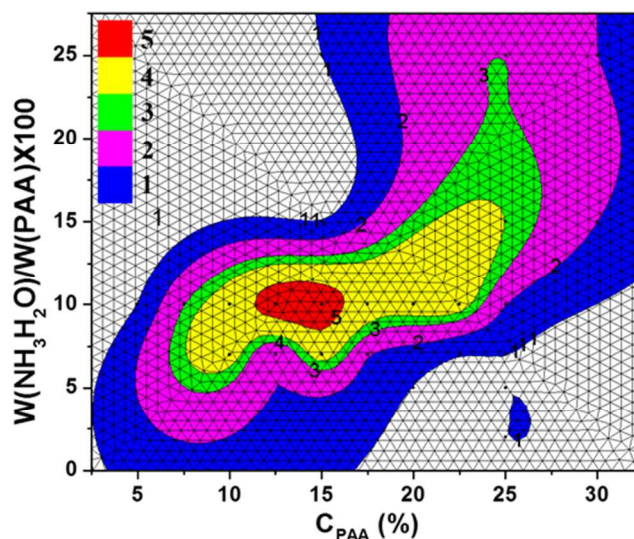
Figure 3. Contour plots the spinnabilities of PAA-salt water solution with different adding amount of ammonia and PAA by electrospinning. The numbers, 1, 2, 3, 4 and 5, are corresponding to the spinnability in Table S1. Red area shows good electrospinning results for samples S24 and S26-28.

TGA analysis. TGA could provide information regarding the thermal decomposition of polymers. In this work, it was used to determine the final imidization temperature and the

thermal stability of the obtained PI nanofibers. As shown in Figure 4, PEO started to decompose at approximately 300 ^{o}C and the char yields at 400 and 466 ^{o}C were 44% and 3%, respectively. The pure precursor of PAA-salt showed two obvious weight loss steps. The first step with about 17% weight loss below 220 ^{o}C could be attributed to the evaporation of residual solvent and the imidization process. The second step started around 561 ^{o}C, which could be due to the decomposition of PI. A weight loss platform was observed between 250 to 500 ^{o}C, suggesting the thermal stable temperature range of PI. Thus, in this work, 400 ^{o}C was chosen as the final imidization temperature and the annealing time was 1 h, by which the PEO was decomposed completely and the PAA and PAA-salt would convert to PI. Pure PAA, PAA-salt, and PAA-salt/PEO nanofibers presented very similar TGA curves. PAA-salt showed 4% smaller char yield at 800 ^{o}C than PAA due to more weight release of NH_4OH from PAA-salt than of H_2O from PAA during the imidization process. When comparing the char yield of PAA-salt and PAA-salt/PEO, PAA-salt/PEO exhibited about 3% smaller than PAA-salt. This 3% difference of char yield proved the amount of PEO addition in PAA-salt during electrospinning very well. After imidization, due to the same chemical structures (Figure 1), both PIs imidized from PAA and from PAA-salt/PEO showed no weight loss below 500 ^{o}C, indicating the similar very high thermal stability and the complete decomposition of PEO during the imidization process.
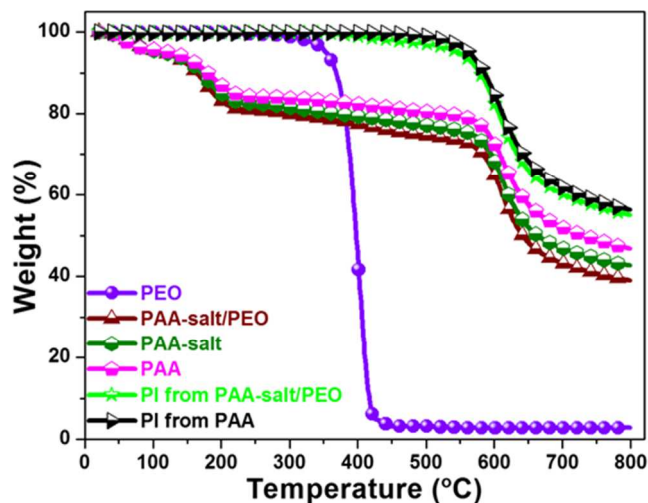
Figure 4. TGA curves of electrospun PAA, PAA-salt/PEO and PI nanofibers, and PAA-salt and PEO powder.

FT-IR analysis. FT-IR spectra were further used to confirm the chemical structures and the thermal conversion to PI from PAA-salt (Figure 5). Due to the quite small amount of PEO in the composite fibers, no obvious signals of PEO appeared in the spectra of PAA-salt/PEO. No differences were observed from the FT-IR spectra of PAA and PAA-salt, which could be owing to the similar chemical structures of PAA and PAA-salt. After high temperature treatment, the characteristic peaks (-NH-; -COOH; C=O, amid I) for PAA and PAA salt disappeared completely and new peaks (C=O, imide I; C-N-C, imide II) appeared, indicating the conversion to PI nanofiber successfully from both PAA and PAA-salt.
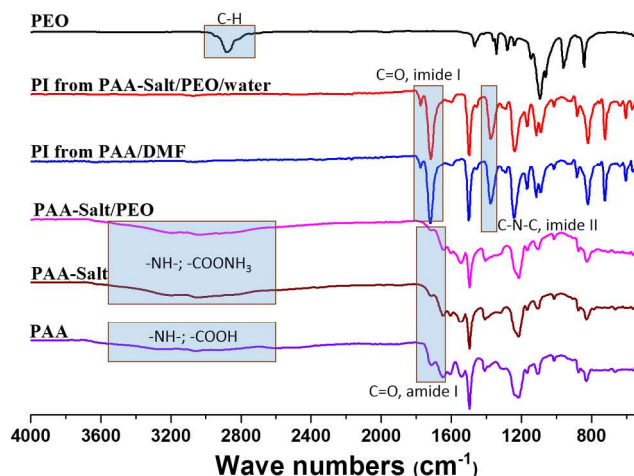
Figure 5. FT-IR spectra of PAA, PAA-salt, PAA-salt/PEO, PI from PAA/DMF, PI from PAA-salt/PEO/water and PEO.

Morphology analysis and water contact angle. The imidization process of PAA-salt/PEO led to a slight decrease of the fiber diameters and the increase of water contact angle (Figure 6). The PAA-salt/PEO nanofibers showed a fiber diameter distribution from 240 to 539 nm with an average fiber diameter of 325 ± 63 nm (Figure 6). After imidization, the PI nanofibers were obtained with fiber diameter distribution from 157 to 522 nm with an average fiber diameter of 295 ± 58 nm (Figure 6). The small shrinkage in fiber diameter from imidization could be due to the complete decomposition of PEO during imidization process. The as-spun PAA-salt/PEO nanofiber mat showed a water contact angle of 90 ± 2 $^{\mathrm{o}}$ (hydrophilic) which increased to $113 \pm 3^{\mathrm{o}}$ after imidization due to removal of ammonia and PEO forming hydrophobic PI nanofibers (Figure 6).
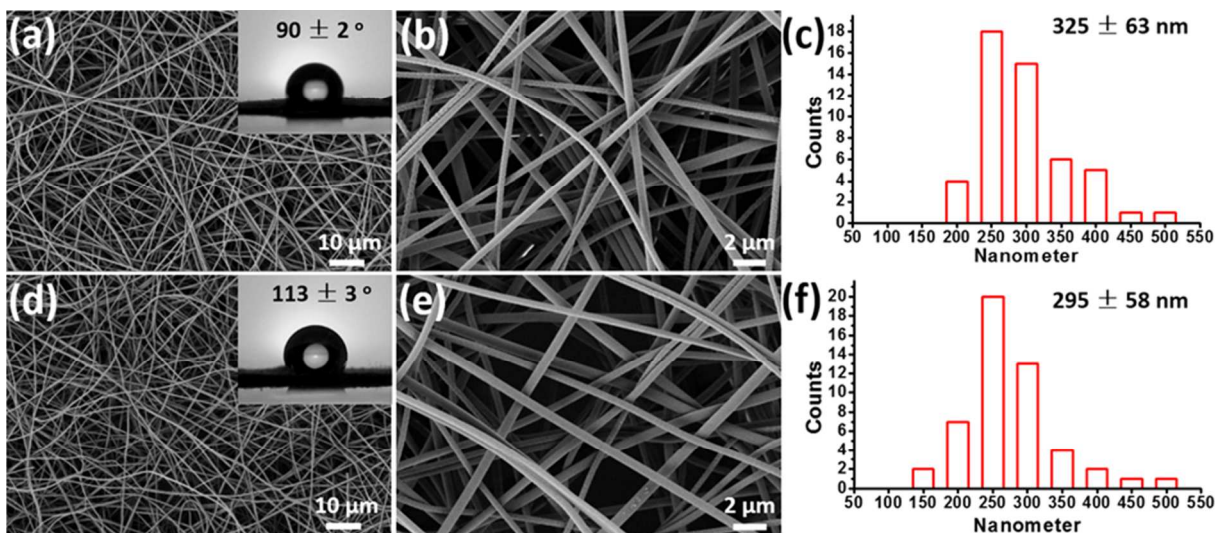
Figure 6. SEM images of electrospun PAA-salt/PEO nanofibers (a, b, sample 26) and PI nanofibers imidized from sample 26 (d, e). (c) and (f) are the fiber diameter distribution of electrospun PAA-salt/PEO and PI nanofibers. Inserts of (a) and (d) are the contact angle of the corresponding PAA-salt/PEO nanofiber mat and PI nanofiber mat.

Stress-strain analysis. Figure 7 depicted the stress-strain curves of electrospun PI nanofiber mats made from PAA-salt/PEO/water solution in comparison to the one made from PAA/DMF solution. The PI mats made from PAA/DMF solution showed an average tensile strength of 79 ± 3 MPa, E modulus of 428 ± 12 MPa, and elongation at break of $22 \pm 2.5\%$. In comparison, the PI mats made from PAA-salt/water showed a decreased tensile strength and E modulus, but slightly higher elongation at break with corresponding average values of 31 ± 1 MPa, 132 ± 9 MPa, and $33 \pm 4.3\%$, respectively. The decrease of tensile strength and E modulus of PI from PAA-salt/water could be due to the nanovoids originated from the decomposition of PEO during imidization process and the more porous and fluffy hierarchical structures of PI mats from PAA-salt/water (Figure 2c) than from PAA/DMF. The higher elongation at break could be attributed

to the higher entanglement of nanofibers in the fluffy PI mats from PAA-salt/water than from PAA/DMF.
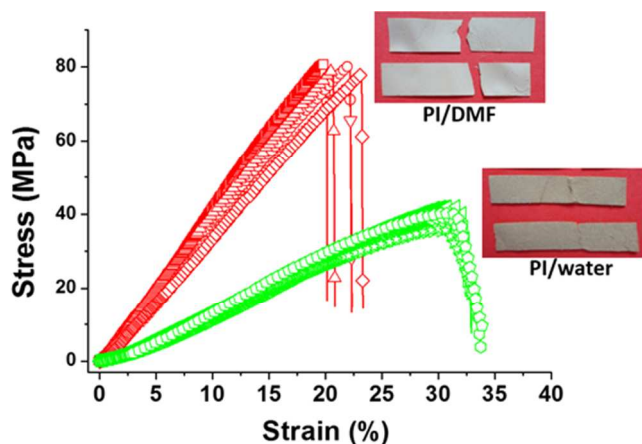

Figure 7. Stress-strain curves of electrospun PI nanofiber mat from PAA/DMF solution and PAA-salt/PEO/water solution respectively. Inserts show the failure fracture structures of the corresponding electrospun PI nanofiber mats.

Aerosol filtration analysis. One of the most relevant applications of PI nanofibers is in filtration. The use of "green" PI nanofibers spun from water for filtration application (aerosol filtration) is compared with PI nanofibers made from DMF (PI/DMF) by depositing them on a steel mesh (support) for different time intervals. Figure 8 showed the morphology of electrospun PI/DMF and PI-salt/water nanofibers on a metal mesh before and after filtration. Both samples showed homogeneous and smooth nanofibers without any beads. With the same electrospinning time of 5 min, it is obvious to observe that the thickness of PI-salt/water nanofibers on the mesh (Figure 8c) was much thinner than PI/DMF nanofibers (Figure 8a), which were matched with the coating densities of 0.889 g/m^2 and 1.07 g/m^2 for PI-salt/water and PI/DMF nanofibers on the mesh, respectively. PI/DMF nanofibers and PI-salt/water possessed an average nanofiber diameter of 245 ± 26 and 287 ± 38 nm, respectively. Filtration efficiency was dependent on the

particle size in the range of 0.2-2.0 μm and the coating densities. As expected, the blank sample, steel mesh supporter, exhibited very poor filtration efficiency below 20% for the whole particle size range (Figure 9). PI/water nanofiber mats showed excellent filtration performance. The filtration efficiency was the same (more than 99.8%) for PI/water and PI/DMF nanofibers for particles bigger than 0.8 μm even with very small coating density (0.889 g/m^2) (Figure 8b and 8d). For achieving very high filtration efficiency for small particles (less than 0.8 μm) the higher coating density was required for PI/water nanofibers. This might be due to the difference in the nature of nanofiber deposition. The fluffy nanofibers obtained from PI-salt spinning from water require more nanofibers for a dense structure (Figure 8a and 8c). More than 98% filtration efficiency was observed for coating density of 3.24 g/m^2 for particle sizes below 0.8 um (99.86, 99.13, and 98.57% for 0.505, 0.305, and 0.198 μm particles, respectively) (Figure 9).
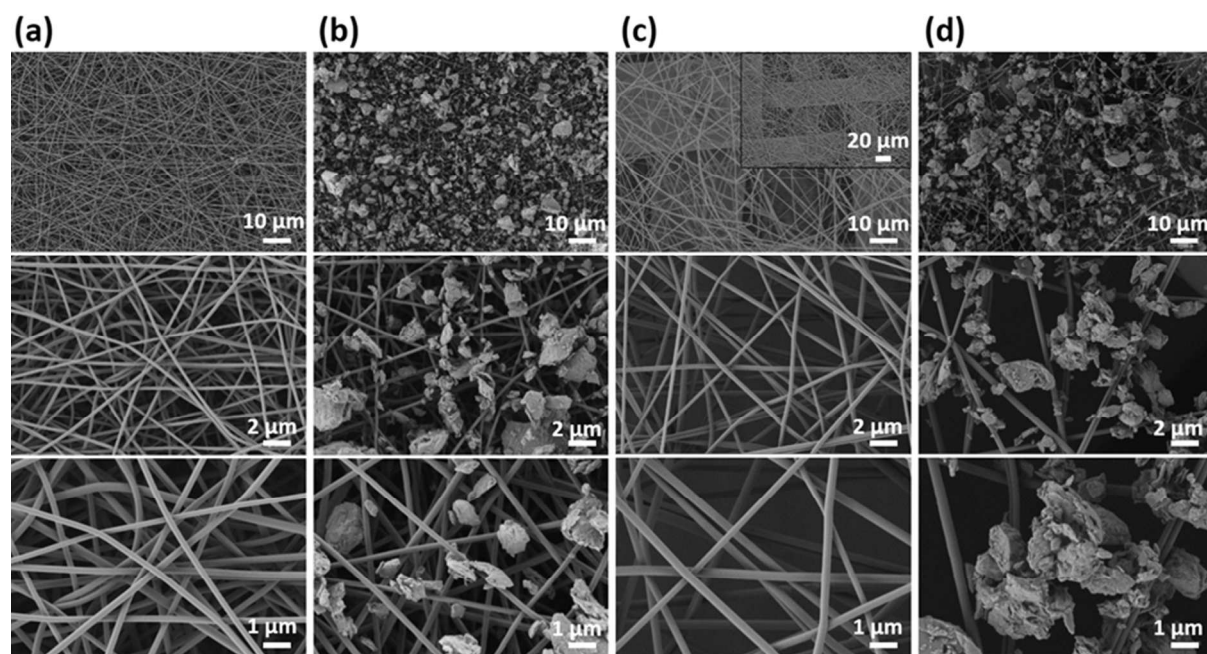
Figure 8. SEM images of electrospun PI mat from PAA/DMF solution (a, b) and PAA-salt/water

solution (c, d) with electrospinning time of 5 min before (a, c) and after (b, d) filtration. Insert of

(c) clearly shows the PAA-salt nanofibers on the steel mesh.
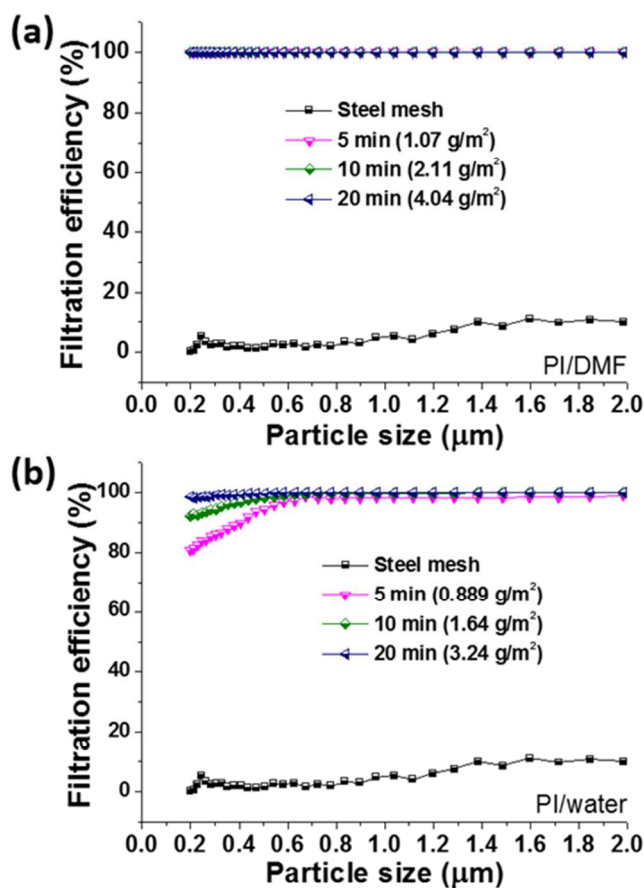
Figure 9. Filtration efficiency of electrospun PI nanofiber mats with different electrospinning

time from PAA/DMF solution (a) and PAA-salt/water solution (b) respectively.

Ashby plot of pressure drop and filtration efficiency. The balance of pressure drop and

filtration efficiency was much better for filters made from PI/water. Interestingly, PI/water mat

showed much better performance in terms of the pressure drop (Figure 10a). The pressure drop

was significantly lower for all samples made from PI/water (24 - 39 Pa) in comparison to the

samples made from PI/DMF (56 - 70 Pa). When comparing the pressure drop of different filter

mediums, the PI/DMF and PI/water mat as filter medium in this research occupied a very important area where the pressure drop is smaller than 100 Pa and the coating density is smaller than 5 g/m^2 (Figure 10a). Quality factor (QF) is an important parameter to evaluate the quality of the filter with the comprehensive evaluation on the filtration efficiency and the pressure drop. The higher values of QF stand for the more efficient filters.[32] In this work, the QF for 300 nm particle size was calculated and a comparison was made with other filter media as shown in the Ashby plot (Figure 10b). Although PI/water filters exhibited a little smaller QF than PI/DMF filters, both filters showed excellent filter quality as the QF was larger than 0.05 Pa^{-1} with the coating density smaller than 5 g/m^2. The QF in this work was larger than most of the filter mediums in the literature, which suggested that PI/DMF and PI/water are ideal candidates as filter mediums in filtration applications. This QF does not even include the temperature stability of PI in comparison to other polymers, which has been demonstrated in the following section for hot liquid filtration.
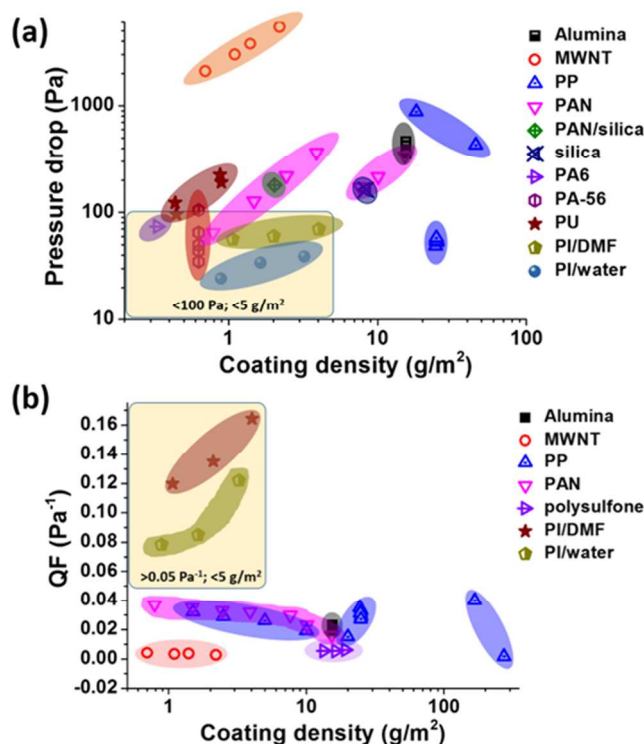
Figure 10. Ashby plot of pressure drop vs coating density (a) and quality factor (QF) VS coating density (b) for various filter media. (Alumina,[33] MWNT,[32] PP,[34-37] PAN,[38-39] PAN/silica,[40] silica,[41] PA6,[42] PA-56,[43] PU,[44] and polysulfone.[45]

Hot liquid filtration. The use of PI-salt/water nanofibers for high temperature filtration is also documented. PI in general is a highly thermally stable polymer with decomposition temperature higher than 500 ^{o}C (Figure 4). In this work, a mixture of Fe_2O_3 and silicon oil was pre-heated up to 200 ^{o}C for filtration using a lab-assembled set-up (Figure 11a). The Fe_2O_3 particles have a size distribution of 1 - 40 μm, which were characterized by SEM (Figure S1). The high temperature filtration was followed by IR-camera, visual inspection of the filtrate, and digital microscope of the filters. When the pre-heated oil was transferred in the funnel, a maximum temperature up to 123.5 ^{o}C on the top of the filtration set-up was observed (Figure 11b) while after filtration, a temperature of 76.6 ^{o}C from the bottom of the filtration set-up was detected by IR camera

(Figure 11b). Due to the heat exchange between the hot oil and the environment and the heat insulation from the glass funnel and the glass filter flask, it is expected that the temperature of the oil in the funnel and filter flask was much higher than the detected temperature by IR camera. The morphology analyses on the mat filter before and after filtration showed that the fine Fe_2O_3 particles were separated and held by the PI/water filter (Figure 11d, e). The filtration efficiency was monitored by the transmittance of the Fe_2O_3/oil mixture before and after filtration (Figure 11f). Before filtration, the Fe_2O_3/oil mixture was reddish brown and the corresponding transmittance was nearly 0%. After filtration, the filtrate became highly transparent and the transmittance was nearly 94%, which possessed nearly the same transmittance as the pure silicone oil. The difference on the transmittance confirmed the highly efficiency of high temperature by the PI/water filters.
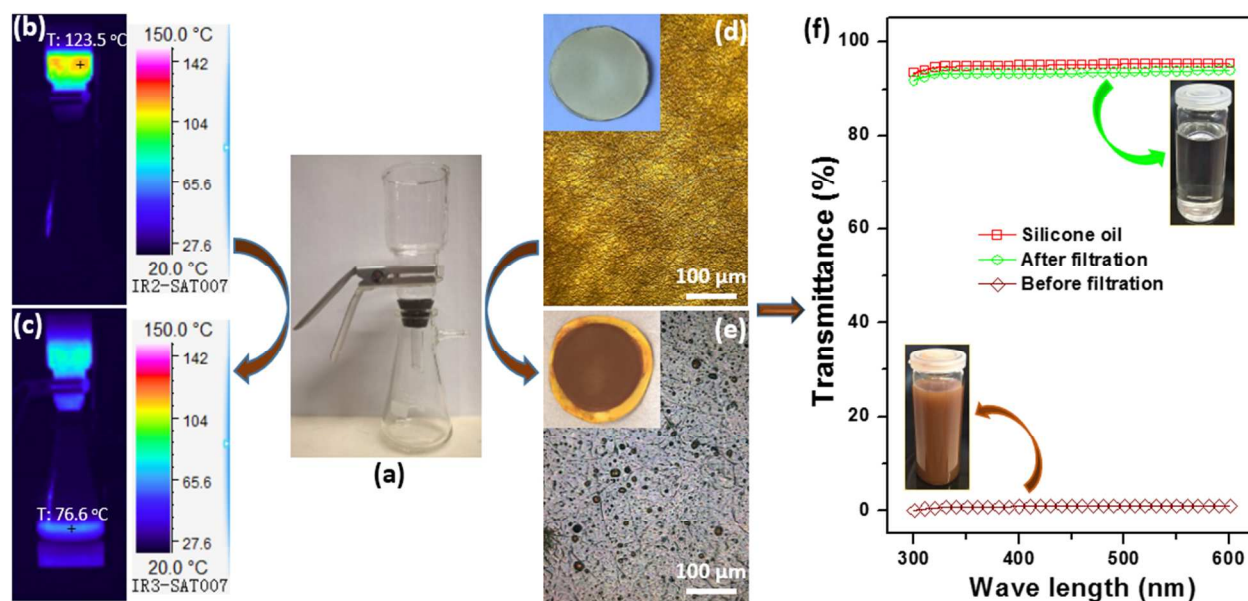
Figure 11. Electrospun PI mat for high temperature filtration. Set-up for high temperature filtration (a), photos of the temperature distribution before (b) and after (c) filtration by IR

camera, photos and digital microscope images of PI mat before (d) and after filtration (e) and transmittance spectra of pure silicone oil and Fe_2O_3/oil mixture before and after filtration (f).

Conclusions

The use of the harmful solvent DMF for the electrospinning of the precursor for polyamide PAA can be now avoided by electrospinning of aqueous solutions of PAA in the presence of well-defined amount of ammonia. The presence of ammonia led to salt formation which inherently increased the conductivity of the solution. The conductivity must be carefully balanced with the viscosity of the solution in order to achieve a stable electrospinning process. Nevertheless, a small amount of water soluble polymer was required in order to provide sufficient viscoelasticity. The PAA-salt fibers obtained from aqueous solution could be converted by thermally induced imidization to PI nanofibers following the standard protocol. The resulting PI nanofiber nonwovens displayed somewhat low mechanical performance as compared to PI nanofiber nonwovens obtained vial electrospinning from DMF solution. Filtration tests with the PI nanofibers nonwovens obtained via aqueous solution showed comparable performance to PI nanofiber nonwovens obtained from DMF solution. High temperature liquid filtration experiments above 100°C showed that the thermomechanical stability of the PI nanofiber nonwovens obtained via aqueous solution was good enough to achieve quantitative filtration of ironoxide microparticles which could be of future interest for oil filtration in engines. In conclusion green electrospinning could be also now applied for high-performance polymers like polyimides, which is encouraging for the electrospinning other high-performance polymer systems.

ASSOCIATED CONTENT

Supporting Information.

Composition of the electrospinning solutions and their electrospinnability; SEM photos Fe_2O_3 particles; data of coating density and pressure drop from different kinds of filter media; data of QF and coating density from different kinds of filter media. "This material is available free of charge via the Internet at http://pubs.acs.org."

AUTHOR INFORMATION

Corresponding Author

*Tel.: +49-921-553399; Fax: +49-921-553393; E-mail: greiner@uni-bayreuth.de

Notes

The authors declare no competing financial interest.

REFERENCES

(1)   Sroog, C. E. Polyimides. *Prog. Polym. Sci.* **1991,** *16* (4), 561-694.

(2)   Ghosh, A.; Banerjee S. Sulfonated fluorinated-aromatic polymers as proton exchange membranes. *e-Polymers* **2014**, *14***,** 227–257.

(3)   Mittal, K. L. Polyimides: synthesis, characterization, and applications. *Springer Science & Business Media* **2013**, *Vol. 1*.

(4)   Ding, M. Isomeric polyimides. *Prog. Polym. Sci.* **2007**, *32* (6), 623-668.

(5)   Tamura, T.; Kawakami, H. Aligned Electrospun Nanofiber Composite Membranes for Fuel Cell Electrolytes. *Nano Lett.* **2010**, *10* (4), 1324-1328.

(6)   Chen, Y.; Han, D.; Ouyang, W.; Chen, S.; Hou, H.; Zhao, Y.; Fong, H. Fabrication and evaluation of polyamide 6 composites with electrospun polyimide nanofibers as skeletal framework. *Composites Part B* **2012**, *43* (5), 2382-2388.

(7)   Miao, Y.-E.; Zhu, G.-N.; Hou, H.; Xia, Y.-Y.; Liu, T. Electrospun polyimide nanofiber-based nonwoven separators for lithium-ion batteries. *J. Power Sources* **2013**, *226*, 82-86.

(8)   Jiang, S.; Duan, G.; Schöbel, J.; Agarwal, S.; Greiner, A. Short electrospun polymeric nanofibers reinforced polyimide nanocomposites. *Compos. Sci. Technol.* **2013**, *88*, 57-61.

(9)   Ye, W.; Zhu, J.; Liao, X.; Jiang, S.; Li, Y.; Fang, H.; Hou, H. Hierarchical three-dimensional micro/nano-architecture of polyaniline nanowires wrapped-on polyimide nanofibers for high performance lithium-ion battery separators. *J. Power Sources* **2015**, *299*, 417-424.

(10)   Agarwal, S.; Jiang, S. Nanofibers and Electrospinning. In *Encyclopedia of Polymeric Nanomaterials*, Kobayashi, S.; Müllen, K., Eds. Springer Berlin Heidelberg **2015**, *Chapter 370-1*, 1323-1337.

(11)   Huang, Z.-M.; Zhang, Y. Z.; Kotaki, M.; Ramakrishna, S. A review on polymer nanofibers by electrospinning and their applications in nanocomposites. *Compos. Sci. Technol.* **2003**, *63* (15), 2223-2253.

(12)   Greiner, A.; Wendorff, J. H. Electrospinning: a fascinating method for the preparation of ultrathin fibers. *Angew. Chem. Int. Ed.* **2007**, *46* (30), 5670-5703.

(13)   Kumar, P. S.; Sundaramurthy, J.; Sundarrajan, S.; Babu, V. J.; Singh, G.; Allakhverdiev, S. I.; Ramakrishna, S. Hierarchical electrospun nanofibers for energy harvesting, production and environmental remediation. *Energy Environ. Sci.* **2014**, *7* (10), 3192-3222.

(14)   Chen, F.; Peng, X.; Li, T.; Chen, S.; Wu, X. F.; Reneker, D. H.; Hou, H. Mechanical characterization of single high-strength electrospun polyimide nanofibres. *J. Phys. D: Appl. Phys.* **2008**, *41*, 025308.

(15)   Chen, S.; Hu, P.; Greiner, A.; Chen, C.; Chen, H.; Chen, F.; Hou, H. Electrospun nanofiber belts made from high performance copolyimide. *Nanotechnology* **2008**, *19* (1), 015604.

(16)   Jiang, S.; Duan, G.; Chen, L.; Hu, X.; Hou, H. Mechanical performance of aligned electrospun polyimide nanofiber belt at high temperature. *Mater. Lett.* **2015**, *140*, 12-15.

(17)   Chen, L.; Jiang, S.; Chen, J.; Chen, F.; He, Y.; Zhu, Y.; Hou, H. Single electrospun nanofiber and aligned nanofiber belts from copolyimide containing pyrimidine units. *New J. Chem.* **2015**, *39* (11), 8956-8963.

(18)   Agarwal, S.; Greiner, A. On the way to clean and safe electrospinning—green electrospinning: emulsion and suspension electrospinning. *Polym. Adv. Technol.* **2011**, *22* (3), 372-378.

(19) Sun, J.; Bubel, K.; Chen, F.; Kissel, T.; Agarwal, S.; Greiner, A. Nanofibers by Green Electrospinning of Aqueous Suspensions of Biodegradable Block Copolyesters for Applications in Medicine, Pharmacy and Agriculture. *Macromol. Rapid Commun.* **2010**, *31*, 2077-2083.

(20)   Bansal, P.; Bubel, K.; Agarwal, S.; Greiner, A. Water-Stable All-Biodegradable Microparticles in Nanofibers by Electrospinning of Aqueous Dispersions for Biotechnical Plant Protection. *Biomacromolecules* **2012**, *13* (2), 439-444.

 (21)   Giebel, E.; Mattheis, C.; Agarwal, S.; Greiner, A. Chameleon Nonwovens by Green Electrospinning. *Adv. Funct. Mater.* **2013**, *23* (25), 3156-3163.

(22)   Bubel, K.; Zhang, Y.; Assem, Y.; Agarwal, S.; Greiner, A. Tenside-Free Biodegradable Polymer Nanofiber Nonwovens by "Green Electrospinning". *Macromolecules* **2013**, *46* (17), 7034-7042.

(23) Bubel, K.; Grunenberg, D.; Vasilyev, G.; Zussman, E.; Agarwal, S.; Greiner, A. Solvent-Free Aqueous Dispersions of Block Copolyesters for Electrospinning of Biodegradable Nonwoven Mats for Biomedical Applications. *Macromol. Mater. Eng.* **2014**, *299* (12), 1445-1454.

(24) Giebel, E.; Getze, J.; Röcker, T.; Greiner, A. The Importance of Crosslinking and Glass Transition Temperature for the Mechanical Strength of Nanofibers Obtained by Green Electrospinning. *Macromol. Mater. Eng.* **2013**, *298*, 439-446.

(25)   Krishnan, R.; Sundarrajan, S.; Ramakrishna, S. Green Processing of Nanofibers for Regenerative Medicine. *Macromol. Mater. Eng.* **2013**, *298* (10), 1034-1058.

(26)   Clemenson, P. I.; Pandiman, D.; Pearson, J. T.; Lavery, A. J. Synthesis and characterization of new water-soluble precursors of polyimides. *Polym. Eng. Sci.* **1997**, *37* (6), 966-977.

(27)   Progar, D. J.; Pike, R. A. Adhesive evaluation of water-soluble LARC-TPI. *Int. J. Adhes. Adhes.* **1988**, *8* (1), 25-32.

(28)   Maekawa, Y.; Miwa, T.; Horie, K.; Yamashita, T. Solution properties of polyamic acids and their amine salts. *React. Funct. Polym.* **1996,** *30* (1–3), 71-73.

(29)   Ding, Y.; Bikson, B.; Nelson, J. K. Polyimide Membranes Derived from Poly(amic acid) Salt Precursor Polymers. 1. Synthesis and Characterization. *Macromolecules* **2002**, *35* (3), 905-911.

(30)   Shayapat, J.; Chung, O. H.; Park, J. S. Electrospun polyimide-composite separator for lithium-ion batteries. *Electrochim. Acta* **2015**, *170*, 110-121.

(31)   Misslitz, H.; Kreger, K.; Schmidt, H.-W. Supramolecular Nanofiber Webs in Nonwoven Scaffolds as Potential Filter Media. *Small* **2013**, *9* (12), 2053-2058.

(32)   Viswanathan, G.; Kane, D. B.; Lipowicz, P. J. High Efficiency Fine Particulate Filtration Using Carbon Nanotube Coatings. *Adv. Mater.* **2004**, *16* (22), 2045-2049.

(33)   Wang, Y.; Li, W.; Xia, Y.; Jiao, X.; Chen, D. Electrospun flexible self-standing [gamma]-alumina fibrous membranes and their potential as high-efficiency fine particulate filtration media. *J. Mater. Chem. A* **2014**, *2* (36), 15124-15131.

(34)   Podgórski, A.; Bałazy, A.; Gradoń, L. Application of nanofibers to improve the filtration efficiency of the most penetrating aerosol particles in fibrous filters. *Chem. Eng. Sci.* **2006**, *61* (20), 6804-6815.

(35)   Shim, W. S.; Leea, D. W. Quality variables of meltblown submicron filter materials. *Indian J. Fibre Text. Res.* **2013**, *38* (2), 132-137.

(36)   Yang, S.; Lee, G. W. M. Filtration characteristics of a fibrous filter pretreated with anionic surfactants for monodisperse solid aerosols. *J. Aerosol Sci.* **2005**, *36* (4), 419-437.

(37)   Hassan, M. A.; Yeom, B. Y.; Wilkie, A.; Pourdeyhimi, B.; Khan, S. A. Fabrication of nanofiber meltblown membranes and their filtration properties. *J. Membr. Sci.* **2013**, *427*, 336-344.

(38)   Zhang, Q.; Welch, J.; Park, H.; Wu, C.-Y.; Sigmund, W.; Marijnissen, J. C. M. Improvement in nanofiber filtration by multiple thin layers of nanofiber mats. *J. Aerosol Sci.* **2010**, *41* (2), 230-236.

(39)   Mei, Y.; Wang, Z.; Li, X. Improving filtration performance of electrospun nanofiber mats by a bimodal method. *J. Appl. Polym. Sci.* **2013**, *128* (2), 1089-1094.

(40)   Wang, N.; Si, Y.; Wang, N.; Sun, G.; El-Newehy, M.; Al-Deyab, S. S.; Ding, B. Multilevel structured polyacrylonitrile/silica nanofibrous membranes for high-performance air filtration. *Sep. Purif. Technol.* **2014**, *126*, 44-51.

(41)   Mao, X.; Si, Y.; Chen, Y.; Yang, L.; Zhao, F.; Ding, B.; Yu, J. Silica nanofibrous membranes with robust flexibility and thermal stability for high-efficiency fine particulate filtration. *RSC Adv.* **2012**, *2* (32), 12216-12223.

(42)   Hung, C.-H.; Leung, W. W.-F. Filtration of nano-aerosol using nanofiber filter under low Peclet number and transitional flow regime. *Sep. Purif. Technol.* **2011**, *79* (1), 34-42.

(43)   Liu, B.; Zhang, S.; Wang, X.; Yu, J.; Ding, B. Efficient and reusable polyamide-56 nanofiber/nets membrane with bimodal structures for air filtration. *J. Colloid Interface Sci.* **2015**, *457*, 203-211.

(44)   Sambaer, W.; Zatloukal, M.; Kimmer, D. 3D air filtration modeling for nanofiber based filters in the ultrafine particle size range. *Chem. Eng. Sci.* **2012**, *82*, 299-311.

(45)   Huang, H.-L.; Yang, S. Filtration characteristics of polysulfone membrane filters. *J. Aerosol Sci.* **2006**, *37* (10), 1198-1208.

For Table of Contents Use Only

Polyimide nanofibers by "Green" electrospinning for air and high temperature filtration

Shaohua Jiang[a], Haoqing Hou[b], Seema Agarwal[a], Andreas Greiner[a]*

[a] Macromolecular Chemistry II, University Bayreuth, Universitätsstraße 30, 95440 Bayreuth, Germany.

[b] Department of Chemistry and Chemical Engineering Jiangxi Normal University, Nanchang, 330022, China.
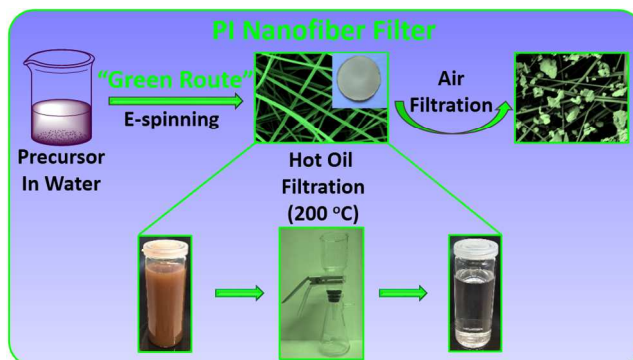
PI nanofibers from water-based precursor by "green" electrospinning are prepared and applied for air and high temperature filtrations.